Optical Materials: X 22 (2024) 100303

Contents lists available at ScienceDirect

Optical Materials: X

journal homepage: www.journals.elsevier.com/optical-materials-x

# Effect of Yb doping on the optical and photoelectric properties of $CsPbCl_3$ single crystals

T.M. Demkiv [a,*], YaM. Chornodolskyy [a], T.M. Muzyka [a], S.Z. Malynych [a,b], R. Ya Serkiz [a], A.S. Pushak [c], A. Kotlov [d], R.V. Gamernyk [a]

[a] Department of Physics, Ivan Franko National University of Lviv, Lviv, Ukraine
[b] Hetman Petro Sahaidachnyi National Army Academy, Lviv, Ukraine
[c] Ukrainian Academy of Printing, Lviv, Ukraine
[d] Photon Science at DESY, Notkestrasse 85, 22607, Hamburg, Germany

ARTICLE INFO

*Keywords:*
Lead-halide perovskites
Single crystal
Quantum cutting effect
Optical properties
Photoelectric properties
Luminescence

ABSTRACT

In this paper, the effect of Yb dopant on the optical and photoelectric properties of $CsPbCl_3$:Yb single crystals is studied. The position of the main energy level of $Yb^{3+}$ ions relative to the energy band was determined. Two channels of electron photoionization into the conduction band were identified, which are photo-stimulated transition of valence electrons and transition of electrons from the ground level of the $Yb^{3+}$ dopant ion. The crucial role of $Yb^{2+}$ ions in the manifestation of the quantum cutting effect was shown. A non-uniform distribution of ytterbium dopant in the $CsPbCl_3$:Yb single crystal volume was revealed. It was established that the absolute quantum yield of ytterbium luminescence in $CsPbCl_3$:Yb single crystals in the near-infrared region at Yb concentration of 2 mol.% reaches 86%.

## 1. Introduction

The growing interest in alkali metal lead-halide perovskites can be attributed to their remarkable properties, such as high luminescence quantum yield, narrow excitonic emission band, large carrier diffusion length, and extended carrier lifetime [1–5]. These distinctive features make these materials highly attractive for numerous potential applications, particularly in optoelectronic devices. This is facilitated by the high color purity of the emission and its tunability throughout the visible spectrum [6]. It has been reported recently that lead halide perovskite nanocrystals were successfully used as a high-performance γ-ray detector [7]. As for the registration of X-ray radiation, ytterbium-doped perovskite nanocrystals are characterized by higher luminescence output than in the most advanced commercially available scintillators [8]. However, structural disorder is observed in the subsurface layer of nanocrystals (with a size below 10 nm) [9], and also electronic processes in nanocrystals substantially differ from those in single crystals. For ytterbium-doped nanocrystals, even up to 20 wt% doping, crystal phase purity is maintained [10], whereas in the work [8] regions with higher impurity concentrations were observed already at a Yb concentration of 5 wt%. In many recent publications, considerable attention has been focused on studies of organic-inorganic compounds, which are particularly attractive for use in the field of photovoltaics [11,12]. At the same time, fully inorganic lead-halide perovskites demonstrate superior stability under diverse environmental conditions, radiation resistance against high-power ultraviolet radiation without photobleaching, and an expanded operational temperature range [13]. It is known that doping alkali metal lead-halide perovskite nanocrystals with trivalent lanthanides, especially ytterbium ions, results in a significant increase in the quantum yield of luminescence in the near-infrared spectral region, exceeding 100% [14–16]. This phenomenon can be rationalized in terms of quantum cutting effect [8,17,18]. In this case, energy is transferred from the perovskite absorption region to the efficient silicon conversion region. Moreover, this energy transfer occurs without energy losses due to the quantum cutting effect, further increasing its efficiency [19].

Taking into account the promising prospects of this tandem approach for future applications, it should be noted that a comprehensive understanding of the energy transfer mechanisms in these crystals is of paramount importance, not only for photovoltaic applications but also for developing high-yield scintillators, emphasizing the quantum cutting effect. In addition, it was shown [20] that ytterbium acts as an efficient sensitizer for erbium excitation in these crystals, involving energy

* Corresponding author.
*E-mail address:* taras.demkiv@lnu.edu.ua (T.M. Demkiv).

https://doi.org/10.1016/j.omx.2024.100303
Received 19 October 2023; Received in revised form 29 January 2024; Accepted 25 February 2024
Available online 7 March 2024

transfer from ytterbium ions to erbium ions. Noteworthy that these conclusions were drawn primarily from nanocrystal studies, whereas in single crystals the processes of local charge compensation upon introducing a non-isovalent trivalent lanthanide impurity may differ [21].

Furthermore, the utilization of such materials in LEDs, photodetectors, solar cells, displays, and lasers primarily depends on the efficiency of charge carrier transfer [22,23]. Therefore, in addition to the optical studies of $CsPbCl_3$:Yb single crystals, conducting a comprehensive analysis of photoelectric processes in these materials is essential to understand the diverse photoionization mechanisms involving impurity and intrinsic defect energy levels. Our present study is focused on the experimentally determining of the energy level positions of ytterbium ions in $CsPbCl_3$:Yb single crystals relative to their energy bands, investigating the luminescence generation mechanism caused by ytterbium ionization, and evaluating the efficiency of energy transfer during photon excitation with energy exceeding the band gap of the studied crystals.

## 2. Experimental

### 2.1. Synthesis

$CsPbCl_3$:Yb single crystals were grown by the Bridgman method using equimolar amounts of separately recrystallized CsCl of purity N4 and $PbCl_2$, purified through zone melting (30 zones) of purity N3. Yb doping was performed using $YbCl_3$; the dopant concentration was determined by the load in the charge. All chemicals were purchased from the company Sigma-Aldrich. The synthesis was conducted in quartz vacuum-sealed ampoules at a pressure $10^{-5}$ Torr; the temperature was kept at 20 °C higher than the melting point for over 12 h. After the growth was completed, the crystals were cooled down to the ambient temperature at a rate of 5 °C per hour. The synthesized crystals appear transparent with a slight yellowish hue.

### 2.2. Optical and photoelectric measurements

Luminescence studies were carried out using synchrotron radiation at the Superlumi/P66 beamline of the PETRA III synchrotron facility at DESY in Hamburg [24]. The desired spectral range of synchrotron radiation for luminescence excitation was selected using a primary 2-m monochromator with a spectral resolution of 4 Å. Luminescence spectra were analyzed using an ANDOR Kymera monochromator with a spectral resolution of 2 Å. The luminescence intensity was recorded using a Newton 920 CCD camera and a Hamamatsu R6358 photomultiplier tube. The samples were obtained through cleaving of the single crystals, the samples were kept at a temperature of 12 K during measurements.

In addition, some measurements of luminescence and reflection spectra were performed at room temperature using a setup based on a 60 cm focal length monochromator. In this case, luminescence excitation was achieved using LED emission (λ = 360 nm, P = 3 W). Quartz halogen lamp was utilized as a light source for measuring reflection spectra.

In order to study carrier dynamics photodiffusion current (PDC) measurements can be used. PDC is the current generated in a sample by external irradiation when no voltage is applied. The measurement of the spectral dependence of the PDC for $CsPbCl_3$:Yb crystal was carried out following the methodology described in Ref. [13]. Additionally, we measured the spectra of photoconductivity in these samples by converting $Yb^{3+}$ impurity to its excited $^2F_{5/2}$ state through additional excitation. The spectra were recorded using synchronous detection according to the schematic shown in Fig. 1.

## 3. Results and discussion

It is known that the energy separation between the ground $^2F_{7/2}$ and the excited $^2F_{5/2}$ states of the $Yb^{3+}$ ion is approximately 1.3 eV [12]. To excite the $Yb^{3+}$ ion, we employed LED radiation (850 nm, P = 3 W) modulated by a mechanical chopper. The photocurrent signal was obtained by illuminating the same spot on the sample's surface with unmodulated monochromatic light. The use of synchronous detection allows recording the photocurrent signal during the presence of the $Yb^{3+}$ ion in the excited $^2F_{5/2}$ state. Thus, the energy of photoionization transitions was determined in the case of the depleted ground $^2F_{7/2}$ level of the $Yb^{3+}$ dopant, namely the transitions that involve energy levels of intrinsic defects and crystal bands, as well as interband transitions.

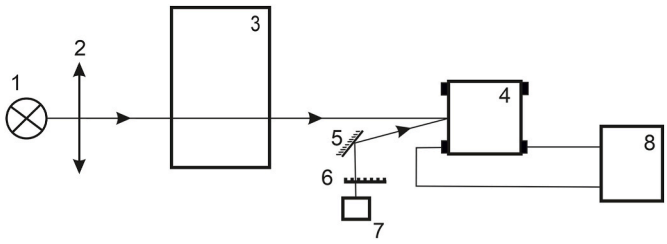


**Fig. 1.** Schematic for the photoconductivity measurements of $CsPbCl_3$:Yb single crystal, where $Yb^{3+}$ ions are excited to $^2F_{5/2}$ state by LED irradiation (λ = 850 nm, P = 3 W). 1 – halogen lamp; 2 – focusing lens; 3 – monochromator; 4 – crystal sample; 5 – mirror; 6 - mechanical chopper; 7 – LED; 8 – synchronous detector.

Fig. 2 depicts the luminescence spectra of the $CsPbCl_3$:Yb crystal at a temperature of 12 K, excited with synchrotron radiation at a wavelength of 160 nm. The emission band at 417 nm corresponds to the luminescence of free excitons, as observed in the undoped crystal. On the other hand, the bands observed in the range of 970–1030 nm are characteristic for $Yb^{3+}$ ion emission [12]. It should be noted that the intensity of $Yb^{3+}$ luminescence in this sample is nearly five times higher compared to the excitonic luminescence. The fine structure of the spectrum can be attributed to the transitions involving spin-orbit split components of $^2F_{5/2}$ level.

The luminescence spectra of the $CsPbCl_3$:Yb single crystal (with Yb concentration $N_{Yb}$ = 5 mol%) at both room and liquid nitrogen temperatures, excited with synchrotron radiation at λ = 160 nm are presented in Fig. 3. The band at 417 nm corresponds to the luminescence of free excitons [25], which is observed in the undoped single crystal and the Yb-doped one at 2 mol% concentration. As can be seen from Fig. 3, the $Yb^{3+}$ ion emission is observed in the range of 920–1050 nm. Additionally, a broad, unstructured band with a peak at 560 nm is also observed in the visible spectral range at 300 K (Fig. 3, a), whose intensity increases in comparison with the spectrum at 80 K (Fig. 3, b).

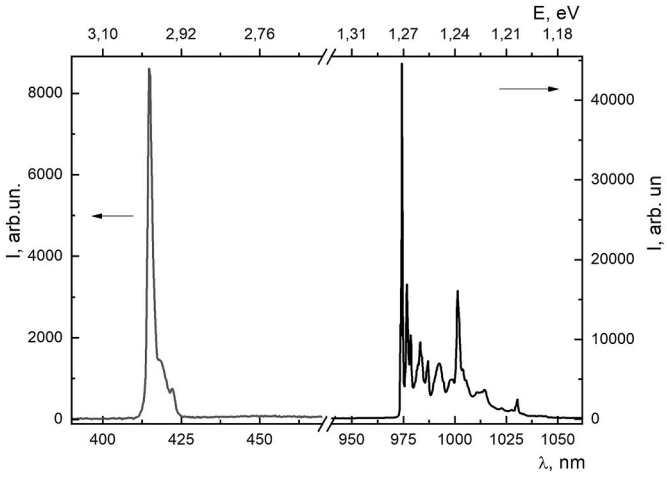


**Fig. 2.** Luminescence spectrum of $CsPbCl_3$:Yb single crystal ($N_{Yb}$ = 2 mol %) at T = 12 K, $\lambda_{exc}$ = 160 nm.

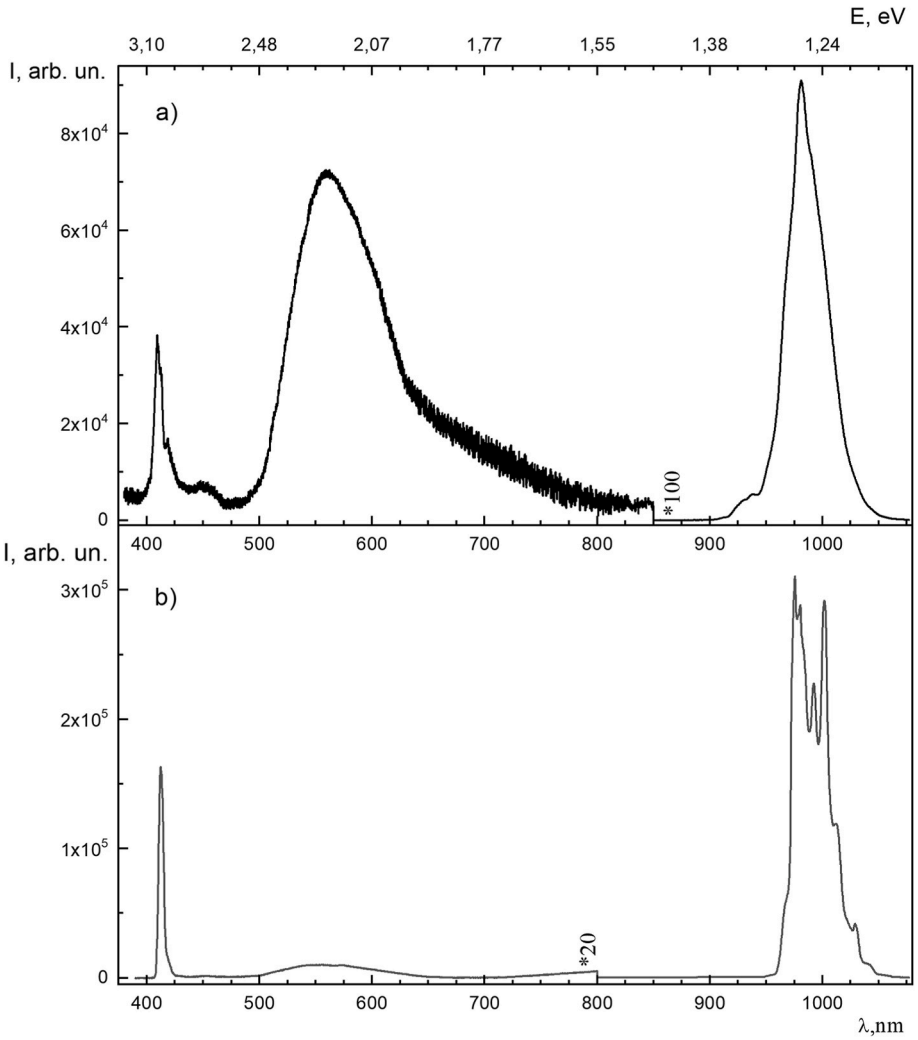


**Fig. 3.** Luminescence spectrum of $CsPbCl_3$:Yb single crystal ($N_{Yb}$ = 5 mol %) at T = 293 K (a) and 80 K (b). $\lambda_{exc}$ = 160 nm.

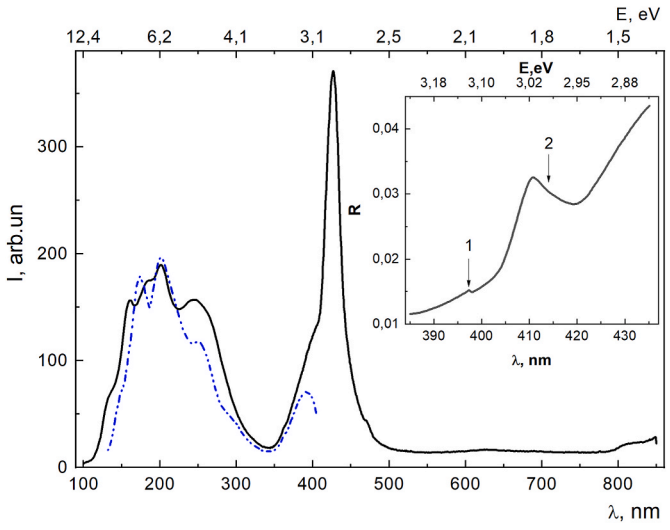


**Fig. 4.** Luminescence excitation spectrum of $CsPbCl_3$:Yb 2 mol% single crystal at T = 293 K, λ = 980 nm band (solid curve) and luminescence excitation spectrum of undoped $CsPbCl_3$ single crystal at T = 12 K, λ = 417 nm band (dashed curve). Inset – reflection spectrum of $CsPbCl_3$:Yb single crystal at T = 293 K.

In Fig. 4, the excitation luminescence spectra of $Yb^{3+}$ ion for the emission band at λ = 980 nm in the $CsPbCl_3$:Yb single crystal at room temperature (solid curve) and for the excitonic luminescence at λ = 417 nm of the undoped $CsPbCl_3$ single crystal at 12 K (dotted curve) are shown. The intense band at 427 nm of the excitation spectrum of $Yb^{3+}$ luminescence in the doped crystal attracts special attention. The presence of a prominent peak at 427 nm in the excitation spectrum of intracenter luminescence for the 980 nm band is somewhat unexpected and can be explained by the efficient capture of photoionized electrons from the $Yb^{3+}$ excited $^2F_{5/2}$ state. This process involves the realization of the quantum cutting effect.

In the inset of Fig. 4, the reflection spectrum of the doped crystal at room temperature is presented. The anomalous dispersion behavior at 414 nm (marked as 2) corresponds to the excitation of free excitons [26]. Note a weakly pronounced feature of anomalous dispersion at 397 nm (marked as 1) whose nature will be discussed later in this article.

Fig. 5 depicts the spectral dependence of the PDC for the $CsPbCl_3$:Yb single crystal. It should be noted that these measurements allow determining the energy and type of photoionization transitions. In the experimental geometry used here, when the photon energy is lower than the band gap (monopolar excitation), bands with positive polarity correspond to electron transitions from the energy levels to the conduction band. At the same time, the band of negative polarity in the band-to-band spectral region indicates the hole-type intrinsic conductivity of the studied single crystal sample. The PDC spectrum (Fig. 5) contains two bands: the band at λ = 427 nm has a positive polarity and

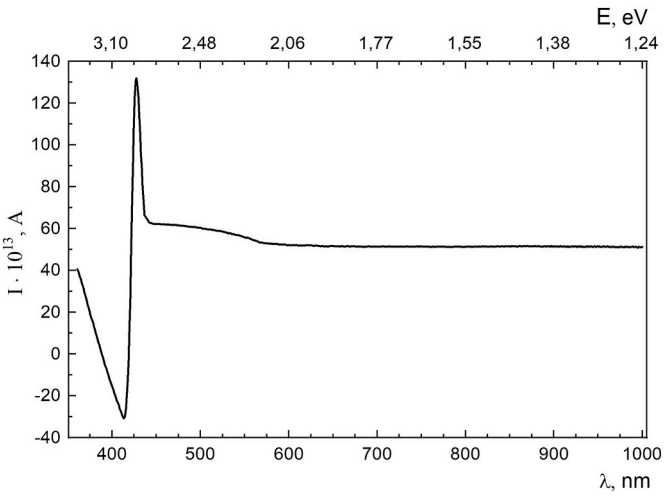


**Fig. 5.** Spectral dependence of photodiffusion current (PDC) of $CsPbCl_3$:Yb single crystal at T = 293 K.

the band at λ = 414 nm a negative polarity. In addition, there is some increase in the intensity of the PDC in the spectral range below 570 nm.

Fig. 6 presents the photoconductivity spectrum of the $CsPbCl_3$:Yb single crystal, when the $Yb^{3+}$ dopant was excited to $^2F_{5/2}$ state using LED emission with a wavelength of 850 nm. In this case an increase in the signal is observed for λ < 570 nm, along with a dip in intensity at λ = 427 nm. Additionally, the bands are observed at 414 nm and 397 nm in the region of λ < 427 nm. Besides, a broad band of low intensity also appears in the spectral region of λ = 830 nm.

It is known that doping of $CsPbCl_3$ single crystals with Yb leads to a slight increase in the crystal's band gap and a remarkable increasing (exceeding 100%) of the quantum yield of $Yb^{3+}$ emission at 980 nm [27]. The structure of luminescence excitation spectra of $CsPbCl_3$:Yb single crystals in the short-wavelength spectral range of (100–400) nm closely resembles that of the undoped $CsPbCl_3$ crystals (Fig. 4, dashed curve) despite substantial temperature differences (300 K and 12 K) during measurements. These observations suggest that the primary excitation mechanism of $Yb^{3+}$ ions is related to energy transfer from the crystal matrix, which can occur through both electron-hole and excitonic processes.

Furthermore, the same spectral positions of the $Yb^{3+}$ ion photoluminescence excitation band at λ = 427 nm (2.904 eV) and the PDC band (Fig. 5) suggest that electron transitions to the conduction band responsible for those spectral features may be associated with the $^2F_{7/2}$ ground state of $Yb^{3+}$ ions. The PDC band at 414 nm (2.994 eV) (see Fig. 5) exhibits a negative polarity and aligns with the exciton excitation band (Inset in Fig. 4, position 2), suggesting exciton dissociation. Similarly, the 397 nm (3.123 eV) band in the PDC spectrum (Fig. 6) with energy that coincide with the region of anomalous dispersion in the reflection spectrum (Inset in Fig. 4, position 1) can be attributed to exciton dissociation in the crystal regions with high Yb concentration. The negative PDC signal in the case of the band-to-band transitions (λ < 409 nm) (Fig. 5) indicates on a hole-type conductivity in the crystal. The increase in the PDC signal for λ < 570 nm (2.17 eV) may be associated with the photoionization of electrons from the local complex level to the conduction band.

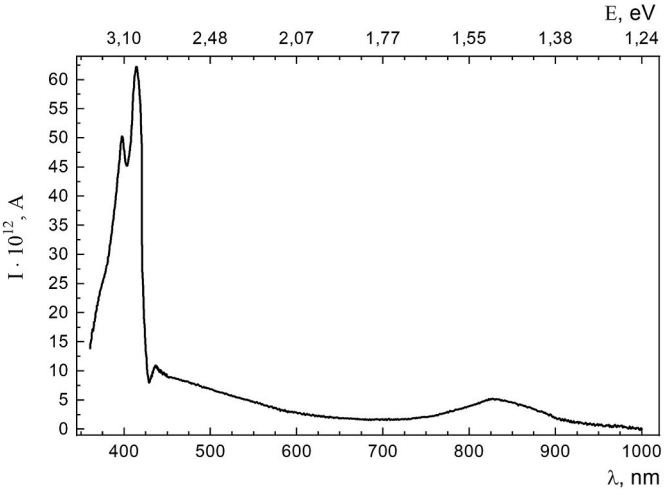


**Fig. 6.** Photoconductivity spectrum of $CsPbCl_3$:Yb single crystal, $Yb^{3+}$ dopant (2 mol %) is excited to $^2F_{5/2}$ state using LED emission with a wavelength of 850 nm.

The exciton excitation band of $CsPbCl_3$:Yb single crystals (Fig. 4, solid curve) is located on the short-wavelength side of the intense band at 427 nm, which corresponds to photoionization transitions of electrons from the $^2F_{7/2}$ ground level of $Yb^{3+}$ ions to the conduction band. The high intensity of the 427 nm band obscures the position of the maximum in the exciton luminescence excitation band, but it can be detected using photoelectric methods. By considering the energy distance between the $^2F_{5/2}$ and $^2F_{7/2}$ states of $Yb^{3+}$ ions (1.265 eV [8,11]) and using intense LED emission (optical power density of ~5 mW/cm$^2$) at 850 nm (E = 1.459 eV), the $Yb^{3+}$ ions were excited from the $^2F_{7/2}$ ground state to the excited $^2F_{5/2}$ state, thus depleting the $^2F_{7/2}$ state. In this case the photoconductivity spectrum at 427 nm, associated with electron transitions from the $2F_{7/2}$ ground state of $Yb^{3+}$ ions to the conduction band, disappears, revealing a small dip in this region (Fig. 6). As a result, the 427 nm band disappears in the photoconductivity spectrum. Instead, a small dip is observed (Fig. 6) in this region. At the same time, a double band with maxima at 414 nm and 397 nm appears in the photoconductivity spectrum, which may be due to the dissociation of excitons formed in regions of the crystal with different concentrations of ytterbium. The excitation energy of excitons in $CsPbCl_3$:Yb single crystals was precisely determined from our optical and photoelectric measurements and amounts E = 2.994 eV (414 nm). Based on the binding energy of excitons 64 meV in the $CsPbCl_3$ single crystal as reported in Ref. [28] and suggesting that this energy remains constant during doping one can estimate the band gap of $CsPbCl_3$:Yb single crystal as 3.059 eV.

According to Ref. [25], in Yb-doped $CsPbCl_3$ crystals, strong Coulomb interaction results in the emerging of uncompensated complexes $(Yb_{Pb} + V_{Pb})^{1-}$ and their clustering followed by the formation of electrically neutral centers $(2Yb_{Pb} + V_{Pb})^0$ that is typical for regions of $CsPbCl_3$:Yb single crystals containing high concentrations of the dopant. The significantly different intensities of the excitonic bands with anomalous dispersion at 414 nm and 397 nm in the reflection spectra (Fig. 4, inset) indicate a heterogeneous distribution of Yb dopants throughout the crystal volume. As previously mentioned, doping of $CsPbCl_3$ single crystal with Yb leads to the increase of the band gap. Therefore, the 397 nm band can be attributed to exciton excitation in regions with high Yb dopant concentration.

The existence of inclusions in a form of $CsPbCl_3$:Yb clusters in the $CsPbCl_3$ matrix is confirmed by elemental composition analysis using EDX (Fig. 7). The probing electron beam with the diameter of ~20 nm allows us to estimate the size of the doped clusters, which do not exceed 1 μm (taking in to account the penetration depth). Similar clusters have been previously observed in our previous studies for $PbI_2$:Mn system [29].

In the regions of the $CsPbCl_3$:Yb single crystal with high dopant concentration, complex electrically neutral centers $(2Yb_{Pb} + V_{Pb})^0$ and complexes $(Yb_{Pb} + V_{Pb})^{1-}$ are formed, where the Yb dopant ion exists in a trivalent state. An increase in the Yb doping concentration results in the appearance of a luminescence band with a maximum at 560 nm. As previously noted, the intensity of this band increases with increasing of the temperature (Fig. 3). A similar band in metal halide perovskites $CsMX_3$ (M = Ca, Sr; X = Cl, Br, I) has been extensively studied in

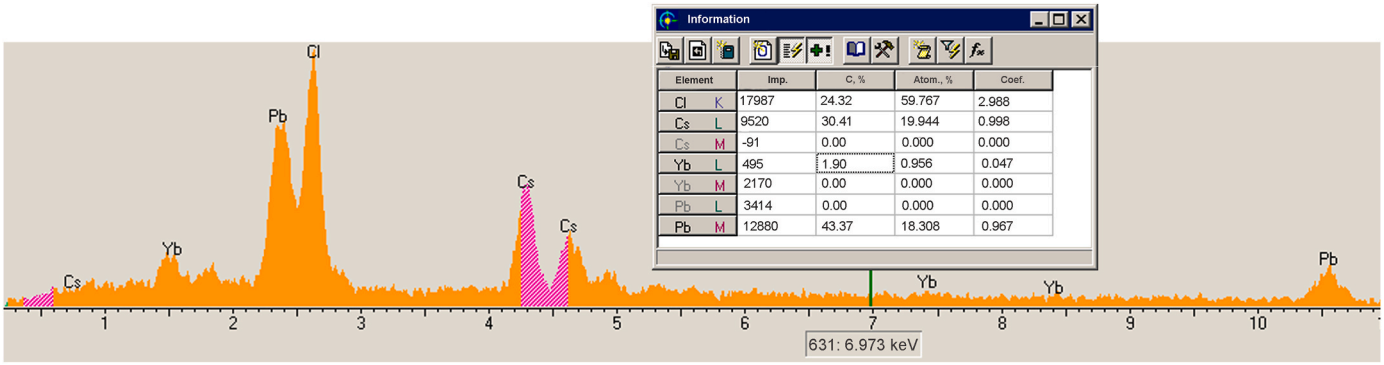


**Fig. 7.** EDX analysis of $CsPbCl_3$:Yb (2 mol.%) single crystal.

Ref. [30] and attributed to $Yb^{2+}$ ion emission. The potential existence of ytterbium in the form of $Yb^{2+}$ ions in metal halide perovskites was considered by Dorenbos [31]. The $Yb^{2+}$ ion is characterized by a completely filled 4*f* shell, thus the excited state of this ion may be associated with $4f^{13}5d^1$ configuration. It should be noted, the energy transition of $4f^{14}\rightarrow 4f^{13}5d^1$ in $Yb^{2+}$ ions coincides with the excitonic emission energy of $CsPbCl_3$:Yb single crystal, facilitating efficient energy transfer from the crystal matrix to $Yb^{2+}$ ions. The luminescence band with a maximum at 560 nm (Fig. 3) corresponds to the spin-allowed $5d^1\rightarrow 4f^{14}$ transitions, while the long-wavelength tail of this band is caused by the spin-forbidden electron transition $5d^1\rightarrow 4f^{14}$ where the forbiddenness is partially weakened due to electron-phonon interactions. Such electron transitions occur within the millisecond range [27].

The observed photoionization transition with energy E = 2.904 eV (427 nm) converts one $Yb^{3+}$ ion to the $(2Yb_{Pb} + V_{Pb})^0$ center containing the $Yb^{4+}$ ions. Since the energy level of $Yb^{3+}$ ion is located 0.155 eV above the top of the valence band, and the energy level of $Yb^{4+}$ ion in the crystal is lower than that of $Yb^{3+}$. Therefore, it falls into the valence band and recharges back to the $Yb^{3+}$ state by capturing an electron. The energy level of $Yb^{2+}$ ion is higher than that of $Yb^{3+}$ and can serve as an efficient trap for excited electrons in the conduction band. Consequently, two pathways for transferring excitation energy from the matrix to $Yb^{3+}$ ions via $Yb^{2+}$ ions exist. As shown in Ref. [29], such energy transfer is particularly effective when the distance between ytterbium ions is close to the exciton Bohr radius, and time of the energy transfer is in the picosecond range. Such a distance between dopant ions is realized in the $(2Yb_{Pb} + V_{Pb})^0$ complex, and the prolonged existence of $Yb^{2+}$ ions in the excited state ensures efficient energy transfer simultaneously to two ytterbium cations and their transition to the $^2F_{5/2}$ state [32]. Quantum cutting is achieved because the band gap is greater than twice the energy between the $^2F_{7/2}$ and $^2F_{5/2}$ excited states of $Yb^{3+}$ ions [33,34]. It was shown [35] that the effective rate of quantum cutting is proportional to the number of Yb dimers, with orthogonal complexes $(2Yb_{Pb} + V_{Pb})^0$ [25] being more efficient than linear ones. As a result, two photons at 988 nm are emitted, doubling the luminescence quantum yield. The integral intensity of this emission increases with temperature [12]. It should be noted that the temperature at which the increase begins (~50 K) attributed to lattice thermal vibrations, providing additional confirmation of the involvement of $Yb^{2+}$ ions in the quantum cutting process. Using an integrating sphere and a non-selective radiometer, the absolute quantum yield of 988 nm emission for the $CsPbCl_3$:Yb single crystal sample (Yb dopant concentration $N_{Yb}$ = 2 mol%) was measured, yielding a value of 86%.

The doping of $CsPbCl_3$ single crystals with ytterbium leads to the formation of various complex centers of the dopant, where lead vacancies contribute to local charge compensation. Each of these centers creates a corresponding energy level within the band gap. The energy of photoionization transitions involving these local levels was precisely determined using photoelectric technique. The combination of photoelectric and luminescence methods made it possible to detect various electron transitions involving ytterbium ions. However, for complete identification of complex centers, additional studies using other methods are needed.

Based on our experimental studies, an energy diagram of the local energy levels of $Yb^{3+}$ ions relative to the energy bands of $CsPbCl_3$:Yb single crystals was constructed as it is shown in Fig. 8. The main energy level of $Yb^{3+}$ dopant ion is located at 0.155 eV above the top of the valence band. The observed 830 nm band in the PDC spectrum corresponds to the transition of valence electrons to the energy level of the $Yb_{Pb}$ + $V_{Pb}$ complex, located at ($E_c$−1.5) eV. The photoionization of electrons from the ($E_c$−2.17) eV level (Fig. 5) to the conduction band corresponds to the electronic process $Yb^{2+} + h\nu = Yb^{3+} + e^-$.

## 4. Conclusions

This work is devoted to the studies of Yb dopant influence on the optical and photoelectric properties of $CsPbCl_3$:Yb single crystals grown by the Bridgman method. The research is aimed on the determination of exact position of the energy level of $Yb^{3+}$ ions relative to the energy bands. The use of mutually complementary optical and photoelectric measurements allows determining the main mechanisms of photoionization of electrons into the conduction band. Two distinct channels of electronic transitions were identified: one involves photostimulated transfer of a valence electron, while the other is due to the transition of

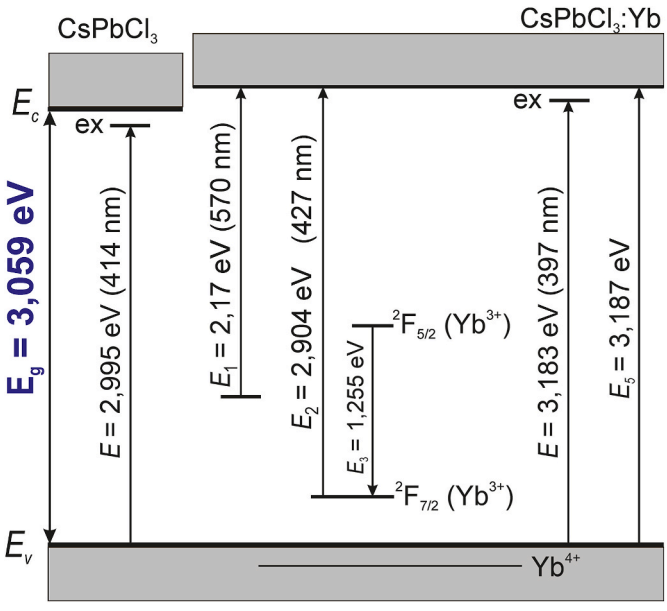


**Fig. 8.** Energy levels and electron transitions in $CsPbCl_3$:Yb single crystal.

electrons from the ground level of $Yb^{3+}$ ions.

The key role of the $Yb^{2+}$ ions in the quantum cutting effect is clearly demonstrated. This effect results in the enhancement in the luminescence efficiency of $CsPbCl_3$:Yb single crystals and has significant implications for the development of advanced optoelectronic devices. Furthermore, a non-uniform distribution of ytterbium dopants within the volume of $CsPbCl_3$:Yb single crystals is revealed. In particular, isolated clusters of $CsPbCl_3$:Yb coexist with the pristine $CsPbCl_3$ matrix, indicating a complex interactions between the dopant ions and the host lattice. These results allow for a deeper understanding of the processes of inclusion of dopants and their diffusion in the crystal structure.

These studies also confirm the influence of ytterbium doping on the band gap of the investigated single crystal. The analysis of the reflection and PDC spectra reveals that the width of the band gap increases as a result of doping of $CsPbCl_3$ crystals by ytterbium. One of the most important outcomes of this research is the determination of the absolute quantum yield of ytterbium luminescence in $CsPbCl_3$:Yb single crystals. In particular, at Yb concentration of 2 mol.%, a quantum yield of 86% was achieved in the near-infrared region. Such a high quantum yield may have significant perspective for various photonic and optoelectronic technologies. In our opinion, findings, presented in this work, not only contribute to the fundamental understanding of such perovskites as $CsPbCl_3$:Yb but also provide an exciting platform for further exploration in the field of optoelectronic materials, in particular, they are very important for the development of metal halide perovskites with special electronic properties for various applications.

## CRediT authorship contribution statement

**T.M. Demkiv:** Conceptualization, Investigation, Writing – original draft, Writing – review & editing. **YaM. Chornodolskyy:** Formal analysis, Funding acquisition, Supervision, Writing – original draft, Writing – review & editing. **T.M. Muzyka:** Funding acquisition, Investigation, Writing – original draft, Writing – review & editing. **S.Z. Malynych:** Formal analysis, Investigation, Supervision, Validation, Writing – original draft. **R. Ya Serkiz:** Methodology, Supervision, Validation, Writing – review & editing. **A.S. Pushak:** Validation, Writing – review & editing. **A. Kotlov:** Methodology, Supervision, Validation, Writing – review & editing. **R.V. Gamernyk:** Conceptualization, Data curation, Formal analysis, Funding acquisition, Investigation, Methodology, Supervision, Writing – original draft, Writing – review & editing.

## Declaration of competing interest

The authors declare that they have no known competing financial interests or personal relationships that could have appeared to influence the work reported in this paper.

## Data availability

Data will be made available on request.

## Acknowledgment

The research leading to this result has been supported by the Ministry of Education and Science of Ukraine within the framework of topic 0122U001860 “Relaxation of electronic excitations in $ABX_3$ type inorganic haloid perovskites” and by the project CALIPSOplus under the Grant Agreement 730872 from the EU Framework Programme for Research and Innovation HORIZON 2020.

## References

[1] D. Shi, V. Adinolfi, R. Comin, M. Yuan, E. Alarousu, A. Buin, Y. Chen, S. Hoogland, A. Rothenberger, K. Katsiev, Ya Losovyj, X. Zhang, P. Dowben, O. Mohammed, E. Sargent, O. Bakr, Solar cells. Low trap-state density and long carrier diffusion in organolead trihalide perovskite single crystals, Science 347 (2015) 519–522, https://doi.org/10.1126/science.aaa2725.

[2] A.A. Zhumekenov, M.I. Saidaminov, A. Md Haque, E. Alarousu, S.P. Sarmah, B. Murali, I. Dursun, X.-H. Miao, A.L. Abdelhady, T. Wu, Formamidinium lead halide perovskite crystals with unprecedented long carrier dynamics and diffusion length, ACS Energy Lett. 1 (2016) 32–37, https://doi.org/10.1021/acsenergylett.6b00002.

[3] J.Y. Kim, J.-W. Lee, H.S. Jung, H. Shin, N.-G. Park, High-efficiency perovskite solar cells, Chem. Rev. 120 (2020) 7867–7918, https://doi.org/10.1021/acs.chemrev.0c00107.

[4] S. Khatoon, S.K. Yadav, V. Chakravorty, J. Singh, R.B. Singh, M.S. Hasnain, S. M. Hasnain, Perovskite solar cell’s efficiency, stability and scalability, A review Materials Science for Energy Technologies 6 (2023) 437–459, https://doi.org/10.1016/j.mset.2023.04.007.

[5] P. Roy, A. Ghosh, F. Barclay, A. Khare, E. Cuce, Perovskite solar cells: a review of the recent, Advances Coatings 12 (2022) 1089, https://doi.org/10.3390/coatings12081089.

[6] L. Protesescu, S. Yakunin, M.I. Bodnarchuk, F. Krieg, R. Caputo, C.H. Hendon, R. X. Yang, A. Walsh, M.V. Kovalenko, Nanocrystals of cesium lead halide perovskites ($CsPbX_3$, X = Cl, Br, and I): novel optoelectronic materials showing bright emission with wide color gamut, Nano Lett. 15 (2015) 3692–3696, https://doi.org/10.1021/nl5048779.

[7] Y. He, C.C. Stoumpos, I. Hadar, Z. Luo, K.M. McCall, Z. Liu, D.Y. Chung, B. W. Wessels, M.G. Kanatzidis, Demonstration of energy-resolved γ-ray detection at room temperature by the $CsPbCl_3$ perovskite semiconductor, J. Am. Chem. Soc. 143 (2021) 2068–2077, https://doi.org/10.1021/jacs.0c12254.

[8] K.A. Dagnall, A.M. Conley, L.U. Yoon, H.S. Rajeev, S.-H. Lee, J.J. Choi, Ytterbium-doped cesium lead chloride perovskite as an X-ray scintillator with high light yield, ACS Omega 7 (2022) 20968–20974, https://doi.org/10.1021/acsomega.2c01712.

[9] L. Piveteau, M. Aebli, N. Yazdani, M. Millen, L. Korosec, F. Krieg, B. Benin, V. Morad, C. Piveteau, T. Shiroka, A. Comas-Vives, C. Copéret, A. Lindenberg, V. Wood, R. Verel, M. Kovalenko, Bulk and nanocrystalline cesium lead-halide perovskites as seen by halide magnetic resonance, ACS Cent. Sci. 6 (7) (2020) 1138–1149, https://doi.org/10.1021/acscentsci.0c00587.

[10] M. Stefanski, V. Boiko, M. Ptak, W. Strek, Effect of $Yb^{3+}$ concentration on the optical properties and trap creation in $CsPbCl_3$ perovskite powder, J. Alloys Compd. 905 (2022) 164216, https://doi.org/10.1016/j.jallcom.2022.164216.

[11] J. Zhang, G. Hodes, Z. Jin, S. Liu, All-inorganic $CsPbX_3$ perovskite solar cells: progress and prospects, Angew. Chem. Int. Ed. 58 (2019) 15596–15618, https://doi.org/10.1002/anie.201901081.

[12] Y.-H. Kim, C. Wolf, Y.-T. Kim, H. Cho, W. Kwon, S. Do, A. Sadhanala, C.G. Park, S. Rhee, S.H. Im, R.H. Friend, T.-W. Lee, Highly efficient light-emitting diodes of colloidal metal-halide perovskite nanocrystals beyond quantum size, ACS Nano 11 (2017) 6586–6593, https://doi.org/10.1021/acsnano.6b07617.

[13] L.-I. Bulyk, R. Gamernyk, Ja Chornodolskyy, T. Malyi, V. Vistovskyy, T. Demkiv, I. Shtablavyi, A. Voloshinovskii, Influence of the degradation processes on luminescent and photoelectrical properties of $CsPbBr_3$ single crystals, J. Alloys Compd. 884 (2021) 161023, https://doi.org/10.1016/j.jallcom.2021.161023.

[14] T.J. Milstein, D.M. Kroupa, D.R. Gamelin, Picosecond quantum cutting generates photoluminescence quantum yields over 100% in ytterbium-doped $CsPbCl_3$ nanocrystals, Nano Lett. 18 (2018) 3792–3799, https://doi.org/10.1021/acs.nanolett.8b01066.

[15] X. Zhang, Y. Zhang, X. Zhang, W. Yin, Y. Wang, H. Wang, M. Lu, Z. Li, Z. Gu, W. Yu, $Yb^{3+}$ and $Yb^{3+}/Er^{3+}$ doping for near-infrared emission and improved stability of $CsPbCl^3$ nanocrystals, J. Mater. Chem. C 37 (2018) 10101–10105, https://doi.org/10.1039/C8TC03957G.

[16] D. Zhou, D. Liu, G. Pan, X. Chen, D. Li, W. Xu, X. Bai, H. Song, Cerium and ytterbium codoped halide perovskite quantum dots: a novel and efficient downconverter for improving the performance of silicon solar cells, Adv. Mater. 29 (2017) 1704149, https://doi.org/10.1002/adma.201704149.

[17] G. Pan, X. Orcid, D. Yang, X. Chen, P. Jing, S. Qu, L. Zhang, D. Zhou, J. Zhu, W. Xu, B. Dong, H. Song, Doping lanthanide into perovskite nanocrystals: highly improved and expanded, optical properties, Nano Lett. 17 (2017) 8005–8011, https://doi.org/10.1021/acs.nanolett.7b04575.

[18] D. Zhou, D. Liu, G. Pan, X. Chen, D. Li, W. Xu, X. Bai, H. Song, Cerium and ytterbium codoped halide perovskite quantum dots: a novel and efficient downconverter for improving the performance of silicon solar cells, Adv. Mater. 29 (2017) 1704149, https://doi.org/10.1002/adma.201704149.

[19] Q. Zhang, X. Huang, Recent progress in quantum cutting phosphors, Prog. Mater. Sci. 55 (2010) 353–427, https://doi.org/10.1016/j.pmatsci.2009.10.001.

[20] M. Zeng, F. Artizzu, J. Liu, S. Singh, F. Locardi, D. Mara, Z. Hens, R. Van Deun, Boosting the $Er^{3+}$ 1.5 μm luminescence in $CsPbCl_3$ perovskite nanocrystals for photonic devices operating at telecommunication wavelengths, ACS Appl. Nano Mater. 3 (2020) 4699–4707, https://doi.org/10.1021/acsanm.0c00701.

[21] C. van Aarle, K. Krämer, P. Dorenbos, Characterization of $Sm^{2+}$-doped $CsYbBr_3$, $CsYbI_3$ and $YbCl_2$ for near-infrared scintillator application, J. Lumin. 251 (2022) 119209, https://doi.org/10.1016/j.jlumin.2022.119209.

[22] Ei Brown, Z. Fleischman, J. McKay, U. Hommerich, Al Kabir, J. Riggins, S. Trivedi, M. Dubinskii, Mid-IR spectroscopy of $Er^{3+}$ doped low-phonon $CsCdCl_3$ and $CsPbCl_3$ crystals, J. Opt. Soc. Am. B 40 (2023) A1–A8, https://doi.org/10.1364/JOSAB.470152.

[23] H. Li, X. Liu, D. Zhou, B. Dong, L. Xu, X. Bai, H. Song, Realization of 1.54-μm light-emitting diodes based on $Er^{3+}/Yb^{3+}$ Co-doped $CsPbCl_3$ films, Advansed Materials 35 (2023) 2300118, https://doi.org/10.1002/adma.202300118.

[24] https://photon-science.desy.de/facilities/petra_iii/beamlines/p66_superlumi/index_eng.html.

[25] O. Pidhornyi, Ya Chornodolskyy, A. Pushak, Y. Smortsova, A. Kotlov, O. Antonyak, T. Demkiv, R. Gamernyk, A. Voloshinovskii, Enhancement of near edge luminescence in cadmium ions doped $CsPbCl_3$ single crystals, J. Appl. Phys. 134 (2023) 135105, https://doi.org/10.1063/5.0159753.

[26] M. Baranowski, P. Plochocka, R. Su, L. Legrand, T. Barisien, F. Bernardot, Q. Xiong, C. Testelin, M. Chamarro, Exciton binding energy and effective mass of $CsPbCl_3$: a magnetooptical study, Photon. Res. 8 (2020) A50, https://doi.org/10.1364/PRJ.401872.

[27] Z. Liu, X. Qin, X. Liu, Luminescence enrichment in perovskite-lanthanide composites: complexity and complementarity Handbook on the, Physics and Chemistry of Rare Earths 61 (2022) 1–29, https://doi.org/10.1016/bs.hpcre.2021.12.002.

[28] D.E. Sommer, D.R. Gamelin, S.T. Dunham, Defect formation in Yb-doped $CsPbCl_3$ from first principles with implications for quantum cutting, Phys. Rev. Mater. 6 (2022) 025404. https://10.1103/PhysRevMaterials.6.025404.

[29] A.P. Bukivskii, I.G. Vertegel, E.D. Chesnokov, P.M. Bukivskij, O.I. Ovcharenko, R. V. Gamernyk, Z.D. Kovalyuk, V.M. Tkach, Yu P. Gnatenko, Formation of $PbMnI_2$ alloys: structural, photoluminescence and nuclear quadrupole resonance studies, J. Alloys Compd. 824 (2020) 153985, https://doi.org/10.1103/10.1016/j.jallcom.2020.153985.

[30] M. Suta, T. Senden, J. Olchowka, M. Adlung, A. Meijerink, C. Wickleder, Decay times of the spin-forbidden and spin-enabled transitions of $Yb^{2+}$ doped in $CsCaX_3$ and $CsSrX_3$ (X = Cl, Br, I), Phys. Chem. Chem. Phys. 19 (2017) 7188–7194, https://doi.org/10.1039/c7cp00581d.

[31] P. Dorenbos, The nephelauxetic effect on the electron binding energy in the $4f^q$ ground state of lanthanides in compounds, J. Lumin. 214 (2019) 116536, https://doi.org/10.1016/j.jlumin.2019.116536.

[32] X. Li, S. Duan, H. Liu, G. Chen, Yi Luo, H. Ågren, Mechanism for the extremely efficient sensitization of $Yb^{3+}$ luminescence in $CsPbCl_3$ nanocrystals, Phys. Chem. Lett. 10 (2019) 487–492, https://doi.org/10.1021/acs.jpclett.8b03406.

[33] D. Zhou, R. Sun, W. Xu, N. Ding, D. Li, X. Chen, G. Pan, X. Bai, H. Song, Impact of host composition, codoping, or tridoping on quantum-cutting emission of ytterbium in halide perovskite quantum dots and solar cell applications, Nano Lett. 19 (2019) 6904–6913, https://doi.org/10.1021/acs.nanolett.9b02139.

[34] A.L. Sunatkari, S.S. Talwatkar, H. Sonawane, A recent development of luminescence properties of $Yb^{3+}$ doped metal halide perovskites nanocrystals for photonic applications: a review, J. Phys.: Conf. Ser. 2426 (2023) 012010, https://doi.org/10.1088/1742-6596/2426/1/012010.

[35] C.S. Erickson, M.J. Crane, T.J. Milstein, D.R. Gamelin, Photoluminescence saturation in quantum-cutting $Yb^{3+}$-doped $CsPb(Cl_{1-x}Br_x)_3$ perovskite nanocrystals: implications for solar downconversion, J. Phys. Chem. C 123 (2019) 12474–12484, https://doi.org/10.1021/acs.jpcc.9b01296.